Effect of Thermal Annealing on the Optical and Morphological Properties of (AETH)PbX_4 (X = Br, I) Perovskite Films Prepared Using Single Source Thermal Ablation

Konstantinos Chondroudis,[†] David B. Mitzi,*[,†] and Phillip Brock[‡]

IBM T. J. Watson Research Center, P.O. Box 218, Yorktown Heights, New York 10598, and IBM Almaden Research Center, 650 Harry Road, San Jose, California 95120

Received August 10, 1999. Revised Manuscript Received October 12, 1999

Films of the new organic−inorganic hybrid materials AETHPbX_4 (AETH = 1,6-bis[5′-(2″-aminoethyl)-2′-thienyl]hexane; X = Br, I) were fabricated using single source thermal ablation (SSTA). The as-deposited films were optically smooth and nominally amorphous. The progressive effects of annealing on the structural, optical, and morphological properties of the films were monitored using powder X-ray diffraction, optical spectroscopy, and atomic force microscopy (AFM). Short duration postdeposition annealing at mild temperatures resulted in well-crystallized films of the AETHPbX_4 hybrid perovskites. It was found that up to some critical annealing temperature (∼120 °C), the emission wavelength and the exciton absorption of the compounds shifted to lower energies as the annealing temperature increased. As confirmed with AFM measurements, this shift in optical properties suggests a gradual increase of the grain size with annealing temperature. When the samples were annealed at higher temperatures (>180 °C) their surface morphology changed dramatically, yielding much rougher surfaces due to substantial grain growth and partial decomposition of the framework (with subsequent loss of the organic component). This work demonstrates that the SSTA method can be combined with postdeposition annealing to fabricate good quality, crystalline organic−inorganic perovskite thin films containing complex organic cations.

I. Introduction

Layered organic−inorganic perovskite materials have recently attracted substantial interest in the literature due to their potential for unique electrical, magnetic, and optical properties.[1] The $(R-NH_3)_2MX_4$ (M = divalent metal, X = halogen) members of the perovskite family comprise the simplest and most numerous examples. By using stoichiometric solvent-based, solid-state, or gas-phase reactions between MX_2 and $R-NH_3X$ salts, each member self-assembles into a multilayer structure in which two-dimensional layers of corner-sharing MX_6 octahedra alternate with layers of aliphatic or single ring aromatic ammonium cations. The ammonium group hydrogen bonds to the inorganic sheet halogens, with the organic tail extending into the space between the layers and holding the structure together via van der Waals interactions. The same layered perovskite structure is also stabilized by diammonium cations, yielding compounds with the general formula $(H_3N-R-NH_3)MX_4$.[1−5] In these systems, there is no van der Waals gap between the layers since the ammonium groups of each organic layer hydrogen bond to two adjacent inorganic layers.

When the metal halide framework comprises group 14 metal halides, the organic−inorganic perovskites are generally analogous to multi quantum well structures, with the semiconducting metal halide sheets alternating with the wider band gap organic layers. Interesting physical properties such as strong room-temperature photoluminescence,[6,7] third-harmonic generation,[8] and polariton absorption[9] arise from excitons in the inorganic sheets. The excitons display large binding energies (>300 meV) and oscillator strength.[6,9] The strong photoluminescence and the ability to tune the emission wavelength by means of incorporating different metal or halogen atoms in the structure make these perovskites attractive as emitter materials in electroluminescent devices, although currently such devices operate only at low temperatures.[10,11] The concept of incorporating organic dye molecules within the perovskite frame-

[†] IBM T.J. Watson Research Center.
[‡] IBM Almaden Research Center.

(1) For a recent review, see: Mitzi, D. B. *Prog. Inorg. Chem.* **1999**, *48*, 1.
(2) Halvorson, K.; Willett, R. D. *Acta Crystallogr. Sect. C* **1988**, *44*, 2071.
(3) Garland, J. K.; Emerson, K.; Pressprich, M. R. *Acta Crystallogr. Sect. C* **1990**, *46*, 1603.
(4) Willett, R. D.; Riedel, E. F. *Chem. Phys.* **1975**, *8*, 112.
(5) Skaarup, S.; Berg, R. W. *J. Solid State Chem.* **1978**, *26*, 59.
(6) Ishihara, T.; Takahashi, J.; Goto, T. *Solid State Commun.* **1989**, *69*, 933.
(7) Papavassiliou, G. C.; Koutselas, I. B. *Synth. Met.* **1995**, *71*, 1713.
(8) Calabrese, J.; Jones, N. L.; Harlow, R. L.; Herron, N.; Thorn, D. L.; Wang, Y. *J. Am. Chem. Soc.* **1991**, *113*, 2328.
(9) Fujita, T.; Sato, Y.; Kuitani, T.; Ishihara, T. *Phys. Rev. B* **1998**, *57*, 12428.
(10) Era, M.; Morimoto, S.; Tsutsui, T.; Saito, S. *Appl. Phys. Lett.* **1994**, *65*, 676.

10.1021/cm990516l CCC: $19.00
Published on Web 12/15/1999

work and the possibility of energy transfer from the inorganic layer, leading to enhancement of the light emission from the dye, has also begun to be considered.[1,12]

If technologically important applications are to be realized, it is essential to obtain these materials in the form of single crystals, or more importantly in the form of thin films. A number of relatively simple thin-film techniques have been demonstrated, including spin-coating,[12,13,14] dip-processing,[15] and dual-source thermal evaporation.[16] While these techniques can be utilized for a number of simple organic−inorganic hybrids, their application is limited for more complex systems (i.e., systems with more complicated and functional organic components). Thin-film deposition using spin-coating, for example, is often hindered by the incompatible solubilities of the organic and inorganic components in a particular solvent. Dual source thermal evaporation often suffers from the difficulty of evaporating the organic salt in a controllable manner, therefore complicating stoichiometric control of the resulting films.

Recently, we communicated the discovery of a fully vacuum compatible technique, single source thermal ablation (SSTA), which involves rapid heating of the organic−inorganic compound using a resistively heated metal sheet as a surface source.[17] The organic−inorganic hybrid is ablated from the metal sheet when a large current is passed through it. The components then redeposit on the substrates, which are positioned above the source. With the use of relatively simple organic components such as phenethylammonium or butylammonium cations and various metal halide frameworks, single-phase, highly ordered, and well-crystallized films are formed. Surprisingly, the correct perovskite structures form without the need for any post-deposition treatment.

The possibility of synthesizing hybrid perovskites containing more complex (and functional) organic components, led us to consider employing thiophene derivatives within the layered perovskite framework, due to their potentially interesting optical properties. For example, the incorporation of the chromophore AEQT [5,5‴-bis(aminoethyl)-2,2′:5′,2″:5″,2‴-quaterthiophene] within a lead(II) halide framework has recently been achieved.[1] Herein, we report on the preparation and optical/morphological characterization of thermally ablated thin films of the new hybrid perovskites, $AETHPbX_4$ {AETH = 1,6-bis[5′-(2″-aminoethyl)-2′-thienyl]hexane; X = Br, I}. Besides examining the SSTA process for these model thiophene-containing compounds, the effect of thermal annealing on the properties of their films is also considered.

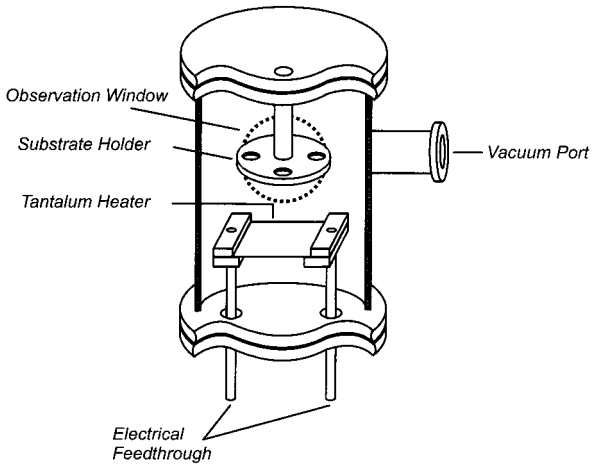

Figure 1. Cross-sectional view of the single source thermal ablation apparatus.

II. Experimental Section

A. Preparation of (AETH)PbX_4 (X = Br, I). The compound $AETHPbBr_4$ was synthesized by first dissolving 0.200 g (0.4 mmol) of AETH·2HBr in 20 mL of methanol and 0.147 g (0.4 mmol) of $PbBr_2$ in 1 mL of concentrated aqueous HBr (48 wt %). Upon dropwise addition of the $PbBr_2$ solution into the AETH·2HBr solution, an off-white precipitate immediately formed. The solution was allowed to cool and then filtered. The yield was typically ∼95%. The compound $AETHPbI_4$ was synthesized similarly, using 0.237 g (0.4 mmol) of AETH·2HI in 10 mL of methanol and 0.184 g of PbI_2 (0.4 mmol) in 1 mL of concentrated aqueous HI (57 wt %). The yield was typically ∼92% of orange crystalline powder. For both compounds the X-ray diffraction patterns for the product were consistent with the lattice constants obtained from a single-crystal structure analysis,[18] indicating a single phase product. Anal. Calcd for $C_{18}H_{30}N_2S_2PbI_4$: C, 20.52; H, 2.87; N, 2.66; S, 6.09. Found: C, 20.61; H, 2.76; N, 2.70; S, 6.12.

B. Thin-Film Deposition and Annealing. The single source thermal ablation apparatus consists of a vacuum chamber, outfitted with an electrical feedthrough, connected to a thin tantalum sheet heater (Figure 1). The substrates were positioned directly above the heater, in an appropriate holder mounted on a z-stage, so that the heater−substrate distance could be selected at will (8 cm for the present work). Quartz substrates were cleaned by sonication in 2% w/v detergent solution in water (20 min), followed by sonication in acetone (20 min), and ethanol (20 min). They were subsequently boiled in ethanol (5 min) and placed in a 130 °C oven to dry. The organic−inorganic hybrid charge may be deposited on the heater by evaporation of a concentrated solution.[17] For poorly soluble materials, however, such as those considered in this report, the best route is to form a thick film on the heater from a suspension in a quick-drying solvent. Accordingly, 0.020 g of $AETHPbI_4$ were placed in 0.7 mL of methanol and sonicated for 15 min until a fine suspension was formed. The charge was then placed dropwise via a syringe on the tantalum heater. The chamber was closed and evacuated with a rotary mechanical pump until all the solvent evaporated (typically about 2 min, as viewed from an observation window attached to the chamber). A turbomolecular pump was then switched on and the system was pumped to $\sim 10^{-7}$ Torr. To initiate the evaporation, a large current of ∼85 A was passed through the heater for about 4 s. It should be noted that during ablation the chamber was isolated temporarily from the pumps (i.e., there was a static vacuum during the process). Ablation occurred in less than 1 s as evidenced by visual observation. The sheet temperature reached ∼1000 °C in 1−2 s, although the charge ablated from the heater well before the latter incandesced. The organic and inorganic components of the

(11) Era, M.; Morimoto, S.; Tsutsui, T.; Saito, S. *Synth. Met.* **1995**, *71*, 2013.
(12) Era, M.; Maeda, K.; Tsutsui, T.; Saito, S. *Chem. Phys. Lett.* **1998**, *296*, 417.
(13) Xu, C.-Q.; Fukuta, S.; Sakahura, H.; Kondo, T.; Ito, R.; Takahashi, Y.; Kumata, K. *Solid State Commun.* **1991**, *79*, 249.
(14) Hattori, T.; Taira, T.; Era, M.; Tsutsui, T.; Saito, S. *Chem. Phys. Lett.* **1996**, *254*, 103.
(15) Liang, K.; Mitzi, D. B.; Prikas, M. T. *Chem. Mater.* **1998**, *10*, 403.
(16) Era, M.; Hattori, T.; Taira, T.; Tsutsui, T. *Chem. Mater.* **1997**, *9*, 8.
(17) Mitzi, D. B.; Prikas, M. T.; Chondroudis, K. *Chem. Mater.* **1999**, *11*, 542.
(18) Mitzi, D. B.; Brock, P.; Dawson, D. J. Unpublished results.

charge sublimed essentially simultaneously and then reassembled on the substrates to form optically clear films. Thickness was controlled by altering the amount of the starting charge that was placed on the heater. The resulting yellow-orange, transparent films were stored in a nitrogen-filled glovebox for further treatment and analysis. Similar conditions were used for the deposition of AETH$PbBr_4$, using a starting charge of 0.025 g suspended in 1 mL of methanol. In this case the resulting films were colorless.

Thermal annealing studies were performed by heating the films on a digitally controlled hot plate placed inside the glovebox. The annealing duration was optimized and found to be ~15−20 min for each temperature considered (50, 80, 100, 120, 150, and 180 °C). When the annealing duration was increased beyond this time frame, no differences in the spectral characteristics were observed. After each anneal, the films were immediately removed from the hot plate and examined using powder X-ray diffraction and optical spectroscopy.

C. X-ray Diffraction. X-ray diffraction patterns were collected at room temperature over the range $3° \leq 2\theta \leq 60°$ using a Siemens D5000 diffractometer (Cu Kα radiation). Because of the reasonable stability of the films, no special precautions for air exposure were taken. The indexing of the diffraction peaks for the AETH$PbBr_4$ sample was performed using the Siemens WIN−INDEX program (exhaustive approach).[19] For the case of AETHPbI_4, indexing was based on a previous single-crystal cell determination.[18] The unit-cell dimensions were refined using the Siemens WIN-METRIC program (least-squares approach), after removing the background and the Cu $K\alpha_2$ component from the diffraction pattern. No change of the diffraction pattern was observed as a result of air or X-ray exposure over the duration of the measurements.

D. Spectroscopic Examination. Fluorescence emission spectra were recorded at room temperature on a SPEX Fluorolog-2 spectrometer using the front-face geometry. Light from a xenon arc lamp was used as the excitation source, after passing it through a SPEX 1680 0.22 m double monochromator. The emitted fluorescence was also passed through a similar double monochromator to a SPEX 1911F detector.

Absorption spectra were obtained on a Hewlett-Packard UV−vis 8543 spectrophotometer at room temperature. Background measurements for the substrates were subtracted from the data.

E. Film Morphological Studies. The topology and microstructure of the annealed films were examined by room-temperature AFM studies, which were performed on a Nanoscope III (DFM-5000, Digital Instruments, Santa Barbara, CA) operating in the tapping mode. Preliminary scan areas were typically 10 × 10 to 50 × 50 μm, with 2 × 2 μm scans for more detailed views.

Films for thickness measurements were deposited through contact shadow masks to form stripes of the material on the substrate. The film thicknesses were measured with a Tencor P-10 stylus profilometer controlled by a personal computer. Measurements were performed over several different areas of each sample. The observed thicknesses ranged between 3500 and 3600 Å for the AETHPbI_4 samples, and between 3700 and 3800 Å for the AETH$PbBr_4$ films.

III. Results and Discussion

The organic molecule (AETH), seen in Figure 2a, consists of two thiophene rings separated by a $-(CH_2)_6-$ segment, which provides for a relatively flexible moiety. Two ethylammonium groups are connected to the 2-positions of each thiophene ring. These groups enable the hydrogen bonding of the molecule to the adjacent perovskite sheets. The molecule was designed[18] with a long, narrow profile to enable the formation of the $(H_3N-R-NH_3)MX_4$ type structure (Figure 2b).

(19) Werner, P.-E. *Z. Kristallorg.* **1964**, *120*, 375.

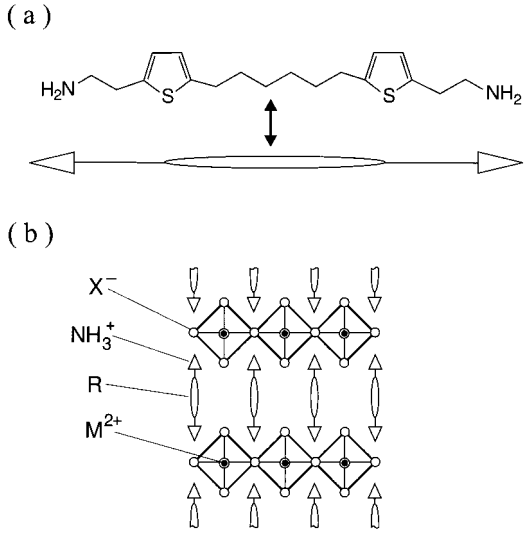

Figure 2. (a) A single 1,6-bis[5′-(2″-aminoethyl)-2′-thienyl]-hexane] molecule (AETH) and (b) schematic representation of the general $(H_3N-R-NH_3)MX_4$ type structure, which consists of sheets of corner-sharing octahedra, interleaved with single layers of diammonium organic cations.

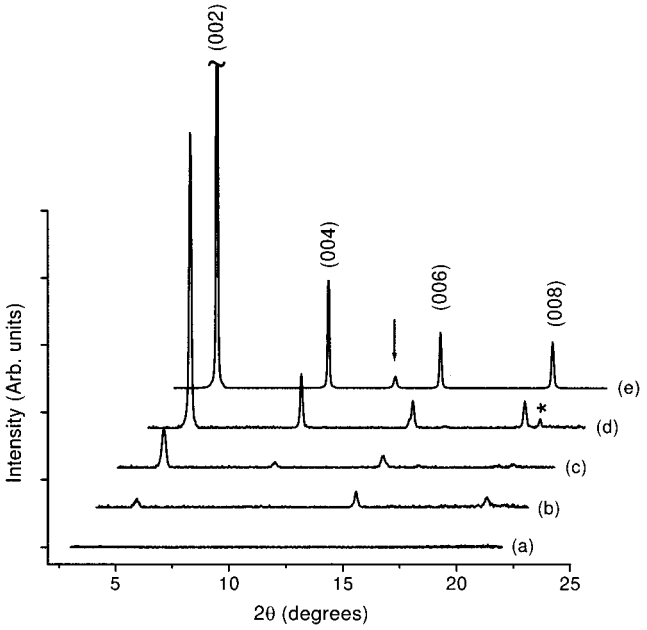

Figure 3. Room-temperature X-ray diffraction patterns of AETHPbI_4 films annealed at different temperatures: (a) no anneal, (b) annealed at 80 °C, (c) at 100 °C, (d) at 120 °C [asterisk (*) indicates the (020) reflection], and (e) at 180 °C [arrow indicates the (001) reflection of PbI_2]. The diffraction patterns have been offset for clarity.

Initially, we attempted preparing thin films of the hybrids using conventional film deposition techniques such as spin-coating and dual-source evaporation. These techniques generally resulted in crystalline films with, however, poor film morphology and/or phase inhomogeneity. Therefore, we attempted to deposit the AETH-PbX_4 films using the SSTA technique. As can be seen in Figure 3a the as-deposited AETHPbX_4 films have an "amorphous" X-ray powder pattern, with no observable X-ray peaks, suggesting a lack of long-range crystalline order. This is in contrast to the as-deposited films obtained when simpler organic molecules were used.[17] A systematic annealing study was undertaken to determine whether the desired crystalline structure could

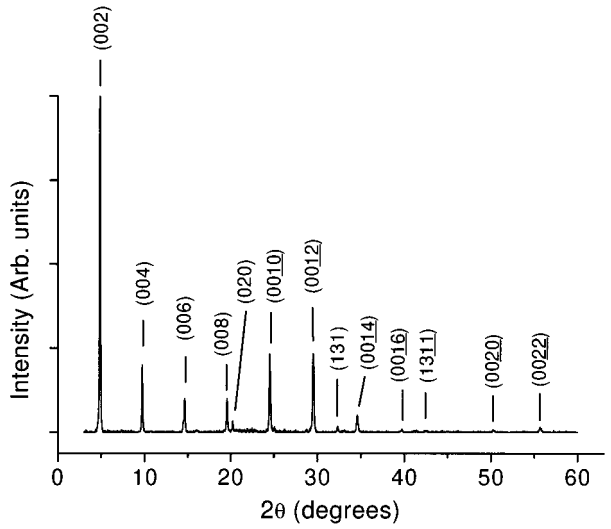

Figure 4. Indexed X-ray diffraction pattern of an $AETHPbI_4$ film annealed at 120 °C.

be induced by thermal annealing and to establish the optimum temperature for such treatment. Low-temperature annealing resulted in the progressive formation of well-crystallized films of the desired product, as evidenced by the presence of higher order peaks in the X-ray diffraction profile (Figure 3). In addition, the films were highly oriented, with the plane of the perovskite sheets parallel to the substrate surface [as indicated by the dominance of the (00*l*) reflections]. Higher annealing temperatures yielded more oriented films, with only (00*l*) reflections observed for films annealed above 120 °C. The optimum annealing temperature was found to be ~120 °C. Above this temperature the films started to slowly decompose, presumably by the decomposition and expulsion of the organic component of the structure. This is supported by the observation of the (001) reflection of PbI_2 at $2\theta = 12.682°$ when the annealing temperature was raised to 180 °C, which clearly indicates that some $AETHPbI_4$ has been converted to PbI_2 through the loss of AETH (see Figure 3e). In an optimally annealed film (120 °C), all 13 of the observed X-ray powder diffraction peaks in the region $3° \leq 2\theta \leq 60°$ indexed to an orthorhombic cell with $a = 8.75(8)$ Å, $b = 8.779(9)$ Å, and $c = 36.311(7)$ Å, indicating a single-phase film (see Figure 4). For the purpose of phase identification and purity it was also compared against that of a crystalline powder of $AETHPbI_4$ and found to be identical. The optical transparency of the films was not preserved for annealing temperatures above 120 °C, mainly due to an increase of the grain size (see below), but also due to partial decomposition at higher temperatures.

The UV−vis spectrum for an unannealed film (Figure 5a) is almost featureless, consistent with the X-ray data, which indicates a lack of long-range crystalline order. However, there is a small shoulder at the wavelength where the excitonic absorption is usually observed (493 nm), hinting at some degree of short-range ordering. Upon annealing, the excitonic absorption gradually increases in intensity while there is a bathochromic shift of about 30 nm in its position (Figure 5b−g, Table 1). This shift is consistent with a gradual increase of the grain size with increasing annealing temperature.

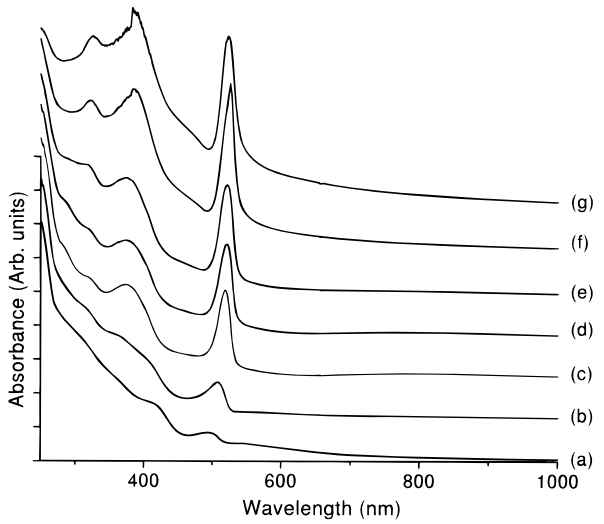

Figure 5. Room-temperature UV−vis spectra of $AETHPbI_4$ films annealed at different temperatures: (a) no anneal, (b) annealed at 50 °C, (c) at 80 °C, (d) at 100 °C, (e) at 120 °C, (f) at 150 °C, and (g) at 180 °C. Peak positions are given in Table 1.

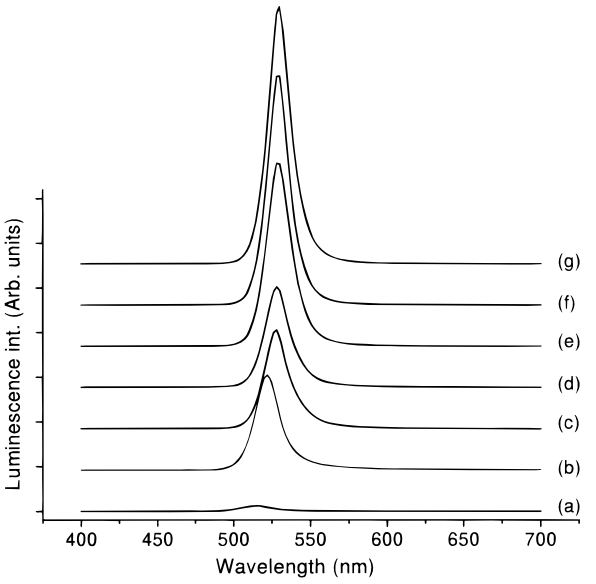

Figure 6. Room-temperature photoluminescence emission spectra of $AETHPbI_4$ films annealed at different temperatures when excited at 375 nm: (a) no anneal, (b) annealed at 50 °C, (c) at 80 °C, (d) at 100 °C, (e) at 120 °C, (f) at 150 °C, and (g) at 180 °C. Peak positions are given in Table 1.

Table 1. Wavelength of Exciton Emission and Absorption as a Function of Annealing Temperature

	no anneal	50 °C	80 °C	100 °C	120 °C	150 °C
emission (nm)	515	522	528	528	529	529
absorption (nm)	493	507	518	520	521	525

The fluorescence emission spectrum for an as-deposited film shows a weak peak located at 515 nm (Figure 6a), consistent with short-range perovskite sheet ordering. The spectra for films annealed at different temperatures are shown in Figure 6b−g. The observed emission peak is due to the radiative decay of excitons in the inorganic sheets and its wavelength is in good agreement with the formation of a two-dimensional lead iodide based perovskite framework.[1,15,20] As for the absorption data, the emission intensity increases with

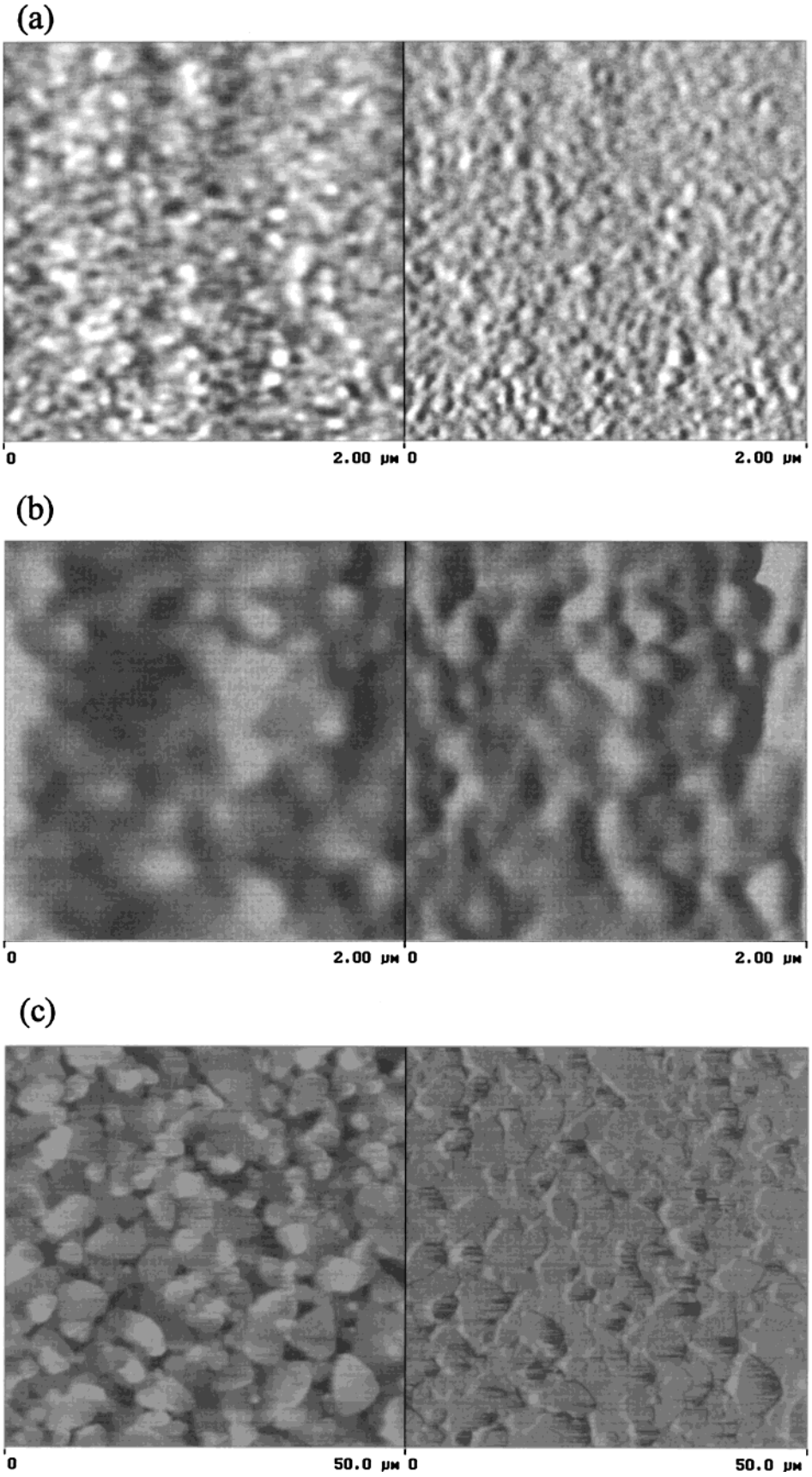

Figure 7. AFM images of $AETHPbI_4$ films annealed at different temperatures: (a) no anneal, (b) annealed at 120 °C, and (c) at 180 °C. The left frames are topology images and the right frames are phase images. Notice the different scale for image c.

the annealing temperature. However, even for as-deposited films, the characteristic green emission was easily observable with the naked eye, when the films were illuminated with a hand-held UV lamp (Mineralight UVGL-25, 365 nm). The room-temperature exciton peak full-width at half-height was around 18 nm,

similar to that observed for well-crystallized organic−inorganic perovskites.[1,22] The emission wavelength shifted to lower energies (515−529 nm) as the annealing temperature increased and stabilized at about 120 °C (Table 1). This is consistent with the shift observed in the absorption spectra and points to a gradual increase of the grain size as the annealing temperature increases. Notice, however, that the fluorescence peak does not shift as much as the absorption peak. The smaller observed Stokes shift with increasing annealing temperature suggests an improvement of the quantum well quality.[23]

To examine the effect of the annealing process on the topology and microstructure of the films, room-temperature AFM studies were performed. The as-deposited films were very smooth, with a mean roughness of 1 nm (Figure 7a). Upon annealing at 80 °C the roughness increased to 2.8 nm (not shown). Further annealing at 120 °C yielded surfaces with a mean roughness of 11 nm (Figure 7b). Although the grain structure was not easily discernible in the AFM images, it was evident that the average surface feature size increased (∼50, 160, 200 nm for no anneal, 80 °C, and 120 °C, respectively), indicating a gradual enlargement of the grain size as the annealing temperature was increased. This is in agreement with the red shift of the absorption and emission spectral characteristics. When the samples were annealed at 180 °C, their surface morphology changed dramatically (Figure 7c). The surface roughness peaked at 72 nm with clearly distinguishable grains. The in-plane grain dimensions varied between 2 and 7 μm. The grain morphology appeared to be mostly platelike, with the plane of the platelets parallel to the substrate surface. This is consistent with the fact that the X-ray powder pattern at this temperature displayed only (00*l*) reflections (Figure 3e). In Figure 7c, the smaller particles appear to have a more random morphology. It is tempting to assume that some of them may be PbI_2 particles produced by the decomposition of $AETHPbI_4$, which is also evident from the X-ray data (as mentioned earlier).

A similar postdeposition treatment for $AETHPbBr_4$ was also successful in producing crystalline films of this compound. The optimum conditions were obtained when the films were annealed at 100 °C for 20 min. All 18 of the observed X-ray powder diffraction peaks in the region $3° \leq 2\theta \leq 60°$ indexed to an orthorhombic cell with $a = 8.203(4)$ Å, $b = 8.305(7)$ Å, and $c = 39.02(2)$ Å, indicating a single-phase film (Figure 8). For the purpose of phase identification and purity it was compared against that of a crystalline powder of $AETHPbBr_4$ and found to be identical. The relatively large number of non-(00*l*) reflections suggests a smaller degree of preferred orientation (i.e., nonparallel orientation of the plane of the perovskite sheets to the substrate surface). The UV−vis spectrum for $AETHPbBr_4$, shown in Figure 9a, displays the characteristic exciton absorption at 413 nm and the luminescence spectrum, shown in Figure 9b, exhibits a strong emission at 418 nm; both

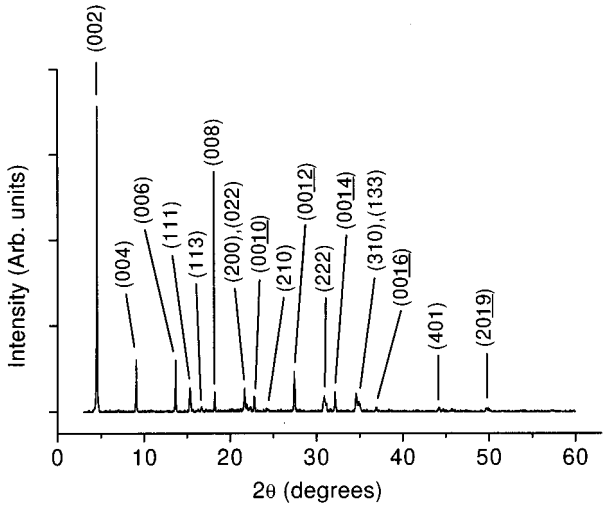

Figure 8. Indexed X-ray diffraction pattern of an $AETHPbBr_4$ film annealed at 100 °C.

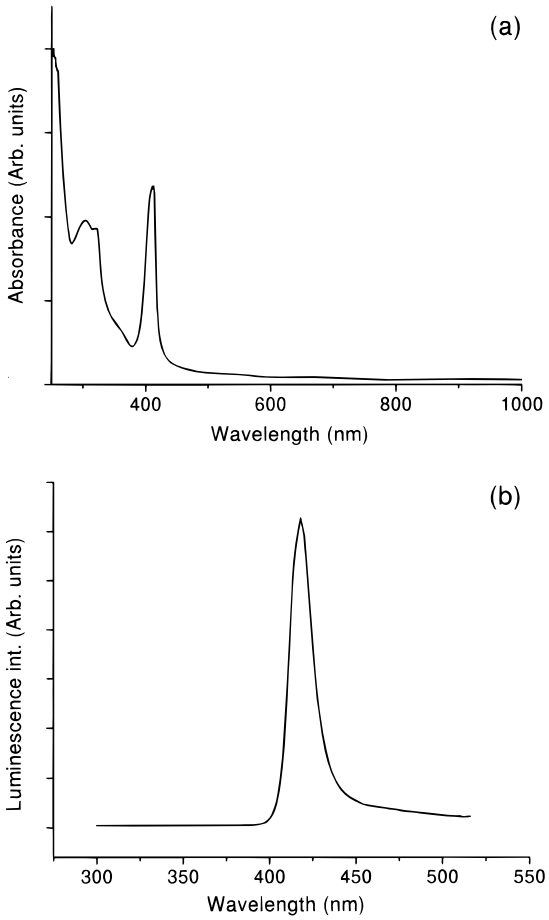

Figure 9. (a) Room-temperature UV−vis spectrum of an $AETHPbBr_4$ film (413-nm peak), and (b) room-temperature photoluminescence emission spectrum (418-nm peak when excited at 325 nm) for the same film. The spectra were obtained from a film annealed at 100 °C.

are consistent with the formation of a well-ordered two-dimensional lead bromide perovskite framework.[1,21]

The crystallization of the $AETHPbX_4$ compounds at relatively mild temperatures and in such a short duration is apparently a manifestation of the self-assembling nature and the high degree of reactivity of these materials. Another example of this reactivity is observed with the dip-processing technique,[15] in which a prede-

(20) Papavassiliou, G. C. *Mol. Cryst. Liq. Cryst. Sci. Technol. Sect. A* **1996**, *286*, 553.
(21) Ishihara, T.; Hirasawa, M.; Goto, T. *Jpn. J. Appl. Phys. Suppl.* **1995**, *34−1*, 71.
(22) Mitzi, D. B.; Liang, K. *Chem. Mater.* **1997**, *9*, 2990.
(23) Papavassiliou, G. C. *Prog. Inorg. Chem.* **1997**, *25*, 125.

posited metal halide film is dipped in a solution containing the organic cations, with reaction between them occurring in seconds to minutes. It appears therefore that a possible model of the SSTA process is the following: during initial deposition, both the organic and the inorganic components leave the heater at about the same time and then reassemble on the substrate in the correct stoichiometry. The films at this stage have very small grain size and the extended quantum well structure is not completely formed. It is interesting to note, however, that even without annealing, there is some evidence of the characteristic exciton peak in the optical spectra, indicating short-range ordering into the sheets of corner-sharing PbX_4 octahedra. Upon annealing, there is gradual rearrangement in the solid state during which the grain size increases. At the optimum temperature, the structure develops to a degree at which exciton emission and absorption are clearly observed, while the X-ray powder pattern indicates a single phase compound, crystallographically oriented with the perovskite sheets mostly parallel to the substrate surface. At elevated temperatures the framework deteriorates, mainly by the decomposition and subsequent loss of the organic component, yielding crystalline metal halide.

Interestingly, whereas crystalline films of $(R-NH_3)_2MX_4$ hybrids containing simple monoammonium organic cations could be deposited using SSTA without further treatment, in the present case, postdeposition annealing was required to obtain crystalline films. As mentioned before, the AETHPbX_4 compounds belong to the $(H_3N-R-NH_3)MX_4$ structure type. The presence of two ammonium groups at the end of the AETH molecule requires that it bonds to the halogens of two adjacent sheets. This renders the molecule less mobile and presumably inhibits the rearrangement in the solid state, resulting in a kinetically stable "amorphous" or microcrystalline phase. By providing additional heat to the system, a gradual transformation can occur to a crystalline phase with progressively larger grain size. The flexibility of the AETH molecule, due to the presence of the $-(CH_2)_6-$ segment, presumably facilitates this rearrangement. Similar studies on organic–inorganic perovskites containing more rigid dye molecules (e.g., AEQT) required higher annealing temperature and/or longer annealing duration.[24]

(24) Chondroudis, K.; Mitzi, D. B. *Chem. Mater.* **1999**, *11*, 3028.

IV. Conclusion

The preparation and characterization of thin films of the new organic–inorganic hybrid materials AETHPbX_4 (AETH = 1,6-bis[5′-(2″-aminoethyl)-2′-thienyl]hexane; X = Br, I) using a single source thermal ablation technique has been achieved. In contrast to simple organic–inorganic hybrids, the incorporation of more complex organic molecules, such as AETH, in crystalline films of the hybrids requires postdeposition annealing. The self-assembling nature and high reactivity of these materials, allows for facile rearrangement in the solid-state and aids in the crystallization of the films during short duration, low-temperature annealing treatments. While as-deposited films were amorphous, well-defined X-ray diffraction patterns were observed in films annealed at temperatures as low as 80 °C. Higher annealing temperatures led to larger grain size within the films until the materials started to decompose near 180 °C. The annealed AETHPbX_4 thin films also demonstrated strong room-temperature exciton absorption and photoluminescence peaks characteristic of well-crystallized layered perovskites.

The solubility of the hybrid is a critical parameter in conventional film preparation methods such as spin-coating or dip-processing. With the current technique there is no dependence of the experimental outcome on the solubility of the hybrid, since suspensions can be used as a starting charge in the SSTA apparatus. Therefore, it becomes feasible to incorporate functional and potentially useful organic molecules and still be able to fabricate good quality thin films. In this respect, we have already demonstrated thin films of the layered perovskite compounds with the AETH cation replaced by the quaterthiophene chromophore AEQT [5,5‴-bis-(aminoethyl)-2,2′:5′,2″:5″,2‴-quaterthiophene].[1,24] In addition, the vacuum compatibility of the technique and the ability to utilize contact masks for the fabrication of patterned films, should facilitate the development of device applications of these materials. The quick turnaround time of the process is also a very desirable feature if industrial applications are to be realized.

Acknowledgment. We are grateful to DARPA for support of this work under contract DAAL01-96-C-0095. We also wish to thank M. Prikas for superior technical assistance, Dr. Richard Murphy for AFM measurements, and Dan J. Dawson for useful discussions.

CM990516L